2021-24-0109 Published 05 Sep 2021

Assessment of a Hydrogen-Fueled Heavy-Duty Yard Truck for Roll-On and Roll-Off Port Operations

Giovanni Di Ilio and Paolo Di Giorgio University of Naples Parthenope

Laura Tribioli University of Rome Niccolò Cusano

Viviana Cigolotti ENEA

Gino Bella University of Rome Niccolò Cusano

Elio Jannelli University of Naples Parthenope

Citation: Di Ilio, G., Di Giorgio, P., Tribioli, L., Cigolotti, V. et al., "Assessment of a Hydrogen-Fueled Heavy-Duty Yard Truck for Roll-On and Roll-Off Port Operations," SAE Technical Paper 2021-24-0109, 2021, doi:10.4271/2021-24-0109.

Abstract

The port-logistic industry has a significant impact on the urban environment nearby ports and on the surrounding coastal areas. This is due to the use of large auxiliary power systems on ships operating during port stays, as well as to the employment of a number of fossil fuel powered road vehicles required for port operations. The environmental impact related to the use of these vehicles is twofold: on one hand, they contribute directly to port emissions by fuel consumption; on the other hand, they require some of the ship auxiliary systems to operate intensively, such as the ventilation system, which must operate to remove the pollutants produced by the vehicle engines inside the ship. The pathway to achieve decarbonization and mitigation of energy use in ports involves therefore the adoption of alternative and cleaner technology solutions for the propulsion systems of such port vehicles.

This paper presents the performance analysis of a hydrogen powered cargo-handling vehicle for roll-on and roll-off port operations in a real case scenario. The fuel cell/battery hybrid powertrain of the vehicle has been previously designed by the authors. On the base of real data acquired during an on-field measurement campaign, and by means of a validated numerical model of the vehicle dynamics, different mission profiles are defined, in terms of driving and duty cycles, in order to represent typical port operations. A rule-based energy management strategy is then used to estimate the energy and hydrogen consumptions required by the vehicle and to assess its suitability to accomplish the defined target port operations. Outputs from this study show the potential of the proposed solution to take the place, in a foreseeable future, of conventional Diesel-engine vehicles, today commonly used in port logistics, towards a zero-emission scenario.

Introduction

Nowadays, 1 billion tons per year of CO_2 emissions - 2.5% of global GHG emissions - are related to shipping in the maritime transport sector [1] and, even in the most optimistic projection, they are estimated to increase by 50% by 2050 [2]. A significant contribution to these emissions can be referred to ships port stays or in-port operations, which now account for around 20 million tons of CO_2 and are expected to increase up to 70 million tons by 2050 [3].

In particular, in-port operations involve a vast number of material handling vehicles of different kind, e.g. yard trucks, forklifts, container movers, rubber-tired gantry cranes, which represent one of the principal sources of emissions in ports, being typically equipped with fossil-fuel based engines, employed both for traction and handling maneuvers. These vehicles require a considerable amount of both available power and on-board stored energy, in order to cope with the power demanding and energy intensive activities they are demanded to, while ensuring an all-day lasting operation, which is characterized by a wide variability of operating conditions and tasks.

Therefore, a green-oriented redesign of such vehicles represents a promising and yet ambitious solution to fasten the decarbonization and energy use mitigation processes in port areas [4]. In the pursuit of this, among all the possible alternatives to be employed for the powertrain of such vehicles, one of the most promising is represented by hydrogen fuel cells (FCs), thanks to their scalability, flexibility and high efficiency, which confer them a high potential, especially when coupled to storage energy devices like Li-ion batteries [5-7].

Hybrid electric powertrains based on FCs have been already widely investigated for heavy-duty vehicle applications

[8-10], but there is a lack of literature dealing with this application in port-logistic vehicles.

For these reasons, the present study investigates the performance of a heavy-duty port Yard Truck (YT), whose original Diesel-based powertrain has been replaced by a hydrogen fuel cell/battery plug-in hybrid powertrain. An experimental campaign on the real Diesel-powered vehicle has allowed the validation of a numerical self-made model of the vehicle, built in Matlab® environment and already proposed by the authors in a previous analysis [11]. Fuel cell and battery sizes, along with powertrain architecture were defined in this study, where a rule-based energy management strategy was implemented and tested for energy and hydrogen consumption estimation. This present paper extends the analysis made in this previous work, where the gearbox was removed from the original driveline and the choice was made to directly connect the electric machine to the transfer case. Here, the effectiveness of using the same transmission of the original vehicle is explored to assess the possibility of reducing the electric motor size with respect to the solution proposed in [11]. In fact, despite the extended speed range of electric traction motors, which usually justifies the omission of a gearbox in electric vehicles, in the present application a gearbox may be useful to increase the wheel torque at low vehicle velocity, thus increasing the maximum road gradient that such vehicles can climb while handling heavy cargos, without the need of oversizing the electric motor. The choice of using the same transmission of the original vehicle is in line with aftermarket powertrain practice, which aims at improving the powertrain efficiency with a minimum number of modifications. Moreover, even if the efficiency of a conventional multi-speed gearbox is most likely lower than the efficiency of an ad-hoc single-speed transmission [12], the potential increase of the overall powertrain efficiency with respect to the Diesel-fueled one is shown to be still ensured. Finally, vehicle performance is estimated under a different set of driving and Roll-on/Roll-off (RoRo) duty cycles, designed and simulated in order to take into account the variability of operating conditions and tasks.

Vehicle Model

A Matlab® self-made quasi-steady backward-looking simulator is employed to model the entire vehicle and identify the potential for energy consumption reduction. The model was validated on data available from the original Diesel-fueled vehicle in [11] and, in this paper, it is further developed by including a gearbox in between the motor and the transfer case. A summary of the main assumptions and governing equations used in the model is reported below.

The model solves the vehicle longitudinal dynamics calculating the traction power (P_t) as per the following Eq. (1):

$$P_t(t) = F_t(t)v(t) = \frac{1}{2}\rho v(t)^3 AC_d + m_v(t)gv(t)\left[f_r(t)cos\theta(t) + sin\theta(t)\right] + \delta m_v(t)a(t)v(t) \quad (1)$$

where $F_t(t)$ is the traction force, $v(t)$ the vehicle speed, ρ the air density (1.2 kg/m^3), A the vehicle frontal area (8 m^2), C_d the drag coefficient (0.8), $m_v(t)$ the vehicle mass, increased by the mass factor δ in the inertia power (i.e. last term) to account for the inertia of the rotating parts of the powertrain, whose value has been set equal to 1.1, $f_r(t)$ the rolling resistance coefficient, g is the gravity acceleration and $\theta(t)$ is the road slope.

In the present application, v obviously changes over time during the mission, but also m_v, θ and f_r are subject to variations along the vehicle driving route and are a function of time. In particular, m_v varies owe to the cargo-handling nature of the vehicle, θ takes into account the slope variation to climb up and down the ramps to the decks of the vessels and f_r varies according to the different pavement characteristics and with the vehicle load during vehicle operations [13, 14]. In fact, the fuel cell/battery hybrid electric vehicle (HEV) proposed in the present study has been derived from a Terberg RT223 YT [15], which is 4x4 heavy-duty yard tractor used in RoRo operations of trailers on ships. The unloaded weight of the original vehicle is about 11.5 t and it is equipped by a Volvo TAD871VE Diesel engine with 185 kW of rated power. For this vehicle, the roll-on operation is characterized by the loading of the trailer in the on-shore terminal area to carry it into the ship, by climbing up/down one or more ramps to the destination deck, where the trailer is unloaded before the truck returns to the on-shore terminal area. Counterwise, in the roll-off operation the truck drives from the on-shore terminal area into the ship with no additional load, climbs up/down one or more ramps to the destination deck, where the trailer is loaded on the truck to bring it to the on-shore terminal area.

In this study, these driving and duty cycles have been varied in order to take into account the mutability of operating conditions and tasks the YT can be demanded to.

In the new powertrain, engine and fuel tank have been replaced by an electric machine (EM) powered by a hydrogen-fueled Ballard FCmove™-HD 70 kW FC [16] and a $LiFePO_4$ battery, as shown in Figure 1. The fuel cell is connected to the EM inverter and battery pack through a DC/DC converter, with an assumed efficiency $\eta_{DC/DC}$ of 93%. The EM is a reversible machine and can receive power for traction from the FC and battery simultaneously or charge the battery during braking or decelerations. At the same time, the FC can provide power both to the EM and the battery, if needed.

Therefore, the total electric power requested to the HEV FC/battery unit is:

$$\begin{cases} P_{tot} = P_{EM}/\eta_{EM} + P_{aux}, & \text{if} \quad P_{EM} \geq 0 \\ P_{tot} = P_{EM}\eta_{EM} + P_{aux}, & \text{if} \quad P_{EM} < 0 \end{cases} \quad (2)$$

FIGURE 1 Powertrain schematic of the fuel cell/battery HEV

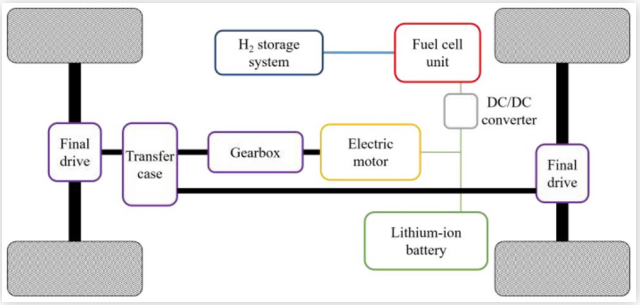

where P_{EM} is the output motor power, η_{EM} is the electric motor efficiency and P_{aux} is the power required by the vehicle accessories, i.e. water pump, cooling fan, air compressor and oil pump, which has been set to 5 kW during the mission, as estimated from the Engine Control Unit (ECU) acquisitions [11].

This total electric power is in turn provided by the fuel cell P_{FC} and the battery P_b, as stated below:

$$P_{tot} = P_{FC}\eta_{DC/DC} + P_b \quad (3)$$

Fuel cell, hydrogen tank and battery sizes, as well as powertrain architecture, have been defined in a previous publication of the authors [11]. Nevertheless, in this present paper, the gearbox of the original vehicle, which was initially removed, has been re-included in the driveline and the electric motor size has been reduced with respect to the solution proposed in [11]. As already mentioned, the gearbox sketched in Figure 1 is the original one, namely an automatic transmission with 6 speeds forward and 3 speeds reverse (ZF, type 6WG211). The overall mechanical transmission efficiency, taking into account all the transmission devices from the EM output to the wheels is a function of the gear number and has been estimated to range from 78% to 85%. In particular, the selected gear number during vehicle operation is retrieved by implementing the actual gear-shift control system of the gearbox, available from private communication with the vehicle manufacturer.

The electric machine used in this investigation is the Danfoss EM-PMI375-T800 [17], a permanent magnet machine whose main characteristics are listed in Table 1, together with a summary of the fuel cell and battery features. All the powertrain components are modeled by means of their performance maps and curves, retrieved from private communications with the manufacturers.

Case Studies Definition: Mission Profiles

The assessment of the hydrogen-fueled heavy-duty YT is conducted on the base of real data acquired during an on-field measurement campaign at the Grimaldi's Terminal located in port of Salerno (Italy) and on the definition of typical mission profiles. Reference driving and duty cycles were retrieved for different YT RoRo port operations for a cargo-vessel having four decks: a *main* deck at the road level, one deck below the main deck (*lower* deck), and two decks above the main deck (*intermediate* and *upper* decks). Specifically, data acquisition was performed for roll-on and roll-off operations at the upper deck and at the lower deck. In all cases, the YT was towing a road trailer, whose weight ranged between 15 t and 30 t.

However, in order to extend the analysis to a more general scenario (the YT towing capacity is up to 70 t), a mathematical model was developed to generate new driving cycles under different operating conditions, that is heavier loads carried by the vehicle. In fact, in the case of higher weights of the trailer, the acquired vehicle speed profiles cannot be truly representative of a realistic scenario, since they would lead to unfeasible power requests, i.e. power requests higher than the maximum allowed by the internal combustion engine (ICE) of the original Diesel-fueled vehicle. Therefore, the developed model starts from an acquired vehicle speed profile and applies local corrections to it whenever the traction power request would exceed the maximum ICE power. The corrected vehicle velocity is obtained by solving the following differential Eq. (4):

$$\eta_t\left(P_{ICE,\max} - P_{aux}\right) - \frac{1}{2}\rho v(t)^3 AC_d$$

$$\frac{dv(t)}{dt}v(t) == \frac{-m_v(t)gv(t)\left[f_r(t)cos\theta(t) + sin\theta(t)\right]}{\delta m_v(t)} \quad (4)$$

where $P_{ICE,\,max}$ is the maximum power output allowed by the ICE and η_t is the overall mechanical transmission efficiency. Eq. (4) is solved by imposing that the total distance travelled by the YT must be the same during both the acquired operation and the one described by the new generated speed profile. Figure 2 shows the obtained vehicle velocity profile related to the roll-on operation at the upper deck of the vessel

TABLE 1 Fuel cell/battery HEV main characteristics. Data taken from [11, 16, 17].

Parameter	Value
EM Max. Continuous torque	938 Nm
EM Rated Torque achieved with one 350A inverter	1300 Nm @ 1900 rpm
EM Nominal efficiency	96 %
FC Rated Power	70 kW
FC Peak Efficiency	57 %
Battery Nominal Energy Capacity, E_b	60 kWh
Battery Max. Peak Discharge C-Rate, C_{rDMp}	5C
Battery Max. Continuous Discharge C-Rate, C_{rDMc}	3C
Battery Max. Peak Charge C-Rate, C_{rCMp}	1.5C
Battery Max. Continuous Charge C-Rate, C_{rCMc}	1C

FIGURE 2 Driving cycles for roll-on port operations at the upper deck, in case of different weights of the trailer

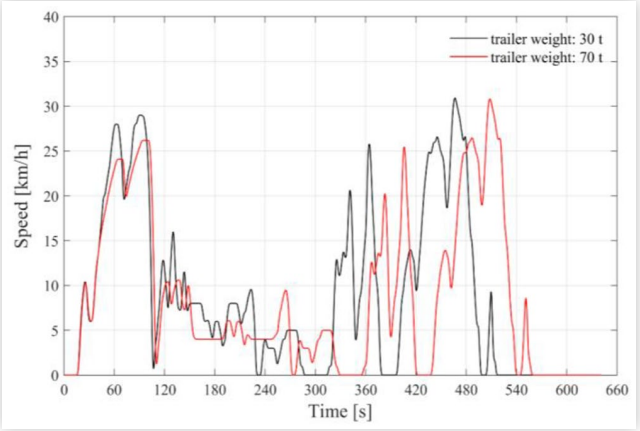

for the YT towing a trailer of 70 t, in comparison with the acquired driving cycle for the same operation conducted by the YT handling a trailer of 30 t.

The generated driving cycle, for the case of 70 t trailer, is consistent with the modeling constraints: during the first stage of the operation, that is when the YT carries the trailer, the obtained velocity is generally lower than the acquired one; in addition, the new driving cycle lasts for around 40 s more than the acquired one, since the traveled distance is the same.

Further driving cycle profiles were also defined in order to consider roll-on and roll-off operations from the intermediate deck, for which no data were available. These cases were simply retrieved by selecting and combining the suitable YT stage operations related to the acquired RoRo at the upper deck.

Table 2 reports all the reference YT operations considered in this study. In particular, cases A-D corresponds to those for which data are available from on-field measurements, and that were also used for the vehicle model validation (already shown in [11] for cases A and B); cases E-H were instead set up upon the validated model and by means of the procedures described above.

Basing on the reference YT port operations, a set of different mission profiles were designed, in order to consider the variability of operating conditions and tasks in the estimation of the vehicle performance, made also for particularly critical operations. The defined mission profiles are reported in Table 3.

All the designed mission profiles last for 6 hours, that is the actual vehicle's range of operation that must be guaranteed.

TABLE 2 Reference YT port operations.

Case	Operation	Weight of the trailer [t]	Time [s]
A	Roll-on upper deck	30	600
B	Roll-off upper deck	15	540
C	Roll-on lower deck	30	480
D	Roll-off lower deck	30	480
E	Roll-on upper deck	70	640
F	Roll-off upper deck	30	540
G	Roll-on intermediate deck	30	480
H	Roll-off intermediate deck	30	480

TABLE 3 Designed mission profiles.

N.	Time [h]	Description	Weight of the trailer [t]
M1	2	Roll-on upper deck	30
	1	Roll-on upper deck	70
	2	Roll-on upper deck	30
	1	Roll-on upper deck	70
M2	3	Roll-off upper deck	30
	3	Roll-on upper deck	30
M3	3	Roll-off intermediate deck	30
	3	Roll-on intermediate deck	30
M4	3	Roll-off lower deck	30
	3	Roll-on lower deck	30
M5	2	Roll-on upper deck	30
	2	Roll-on intermediate deck	30
	2	Roll-on lower deck	30
M6	2	Roll-off upper deck	30
	2	Roll-off intermediate deck	30
	2	Roll-off lower deck	30

Energy Management Strategy

The hydrogen-fueled vehicle is a plug-in vehicle and a rule-based control algorithm, with a feedback control on battery State of Charge (SoC), has been chosen for the in-vehicle power split between the fuel cell and battery to provide the requested P_{tot} as per Eq. (3).

In particular, the energy stored in the battery is exploited according to a Charge Depleting/Charge Sustaining (CD/CS) strategy [18]. To this aim the battery is initially depleted by running the vehicle as a battery electric vehicle, until the predefined threshold of 30% SoC is reached (i.e. CD operation), then the fuel cell/battery system is controlled so as to perform a hysteresis cycle between two predefined levels of SoC (i.e. CS operation), distinguishing two different modes of operation of the powertrain, namely Charging Mode (CM) and Discharging Mode (DM):

1. The first time a SoC equal to 30% is hit, the CM is activated and held until the upper threshold of 40% SoC is reached. In this mode, the fuel cell is the primary energy source, providing power to the EM for traction and to restore the battery SoC to the upper threshold of 40%. In particular, P_{FC} is set to a constant value, given by:

$$P_{FC} = \frac{E_b C_{rCMc}}{\eta_{DC/DC}} = 64.5\,kW \tag{5}$$

The battery is charged both during traction and regeneration, unless the instantaneous motor power request exceeds the value of the fuel cell power given by Eq. (5), leading to a positive value of P_b in the power balance of Eq. (3) that implies battery discharge.

Eq. (5) holds until the battery power is lower than the maximum power the battery can absorb without any damage, corresponding to a maximum peak charge C-rate of 1.5C (see Table 1). If this event occurs, the fuel cell power is reduced to:

$$P_{FC} = \frac{P_{tot} + E_b C_{rCMp}}{\eta_{DC/DC}} \tag{6}$$

2. As soon as the SoC threshold of 40% is hit again, the DM is activated and held until the lower threshold of 30% is reached. In this mode, the battery is the primary energy source to provide power to the EM for traction. Eq. (3) still applies, but P_{FC} is set to a constant value which is significantly reduced with respect to Eq. (5) and is equal to the value

corresponding to the maximum efficiency of the FC (Ballard Power Systems, private communication).

The battery can be still charged during this mode of operation, but only in regenerative mode or if the instantaneous motor power request is lower than the fuel cell power, leading to a negative value of P_b in Eq. (3) that implies battery charge.

It is also worth noting that, if the hydrogen tank is emptied while one of these modes is operating, the CD mode is again activated until a final SoC of 30% so as to ensure the use of all the residual energy in the battery.

Results

First, each reference port operation (Table 2) is simulated, in order to evaluate power and energy demands and to assess the suitability of the selected electric motor along with the proposed driveline configuration. Hence, the vehicle performances, in terms of energy and fuel consumptions, to accomplish the defined mission profiles (Table 3) are evaluated. The results from these analyses are presented in this Section.

Reference Cycles

The electric motor operating points, in terms of speed and torque, are evaluated basing on the estimated electric motor power output and a real-time gear shifting mechanism. The electric motor efficiency profile is then retrieved from its map. As illustrative examples, Figures 3 and 4 show the operating points obtained for cases C and E, respectively. Similar operating point distributions are obtained for all the other cases.

The results indicate that, even in the most critical scenario, that is the roll-on of a 70 t trailer to the upper deck of the vessel (case E), the selected electric motor operates efficiently in its regular working area. This confirms that the proposed driveline configuration with the same gearbox of the original vehicle is a suitable choice.

Next, in Figures 5-8 the total electric power requested to the HEV powertrain (P_{tot}) is presented for all the considered cases,

FIGURE 3 Electric motor operating points in the torque-speed plane, for case C (roll-on to the lower deck, with a 30 t trailer)

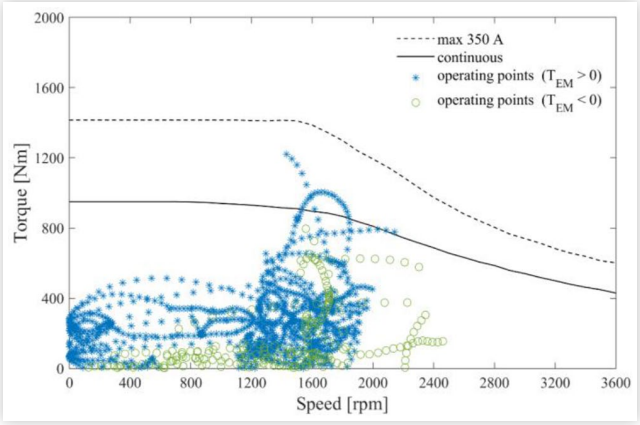

FIGURE 4 Electric motor operating points in the torque-speed plane, for case E (roll-on to the upper deck, with a 70 t trailer)

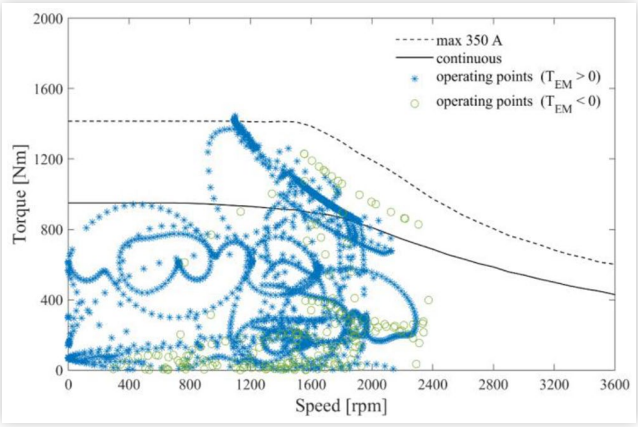

FIGURE 5 HEV total power demand during the driving cycle for cases A and F

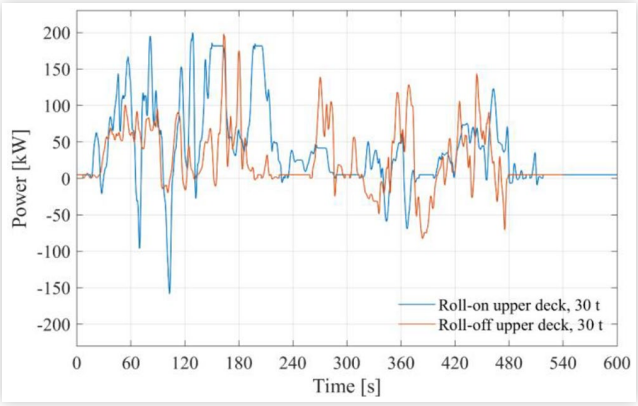

FIGURE 6 HEV total power demand during the driving cycle for cases G and H

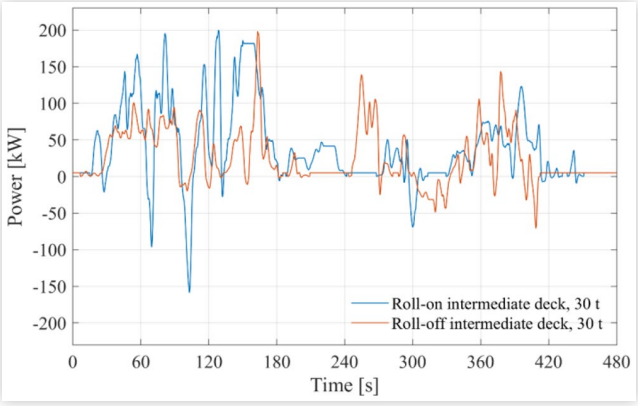

FIGURE 7 HEV total power demand during the driving cycle for cases C and D

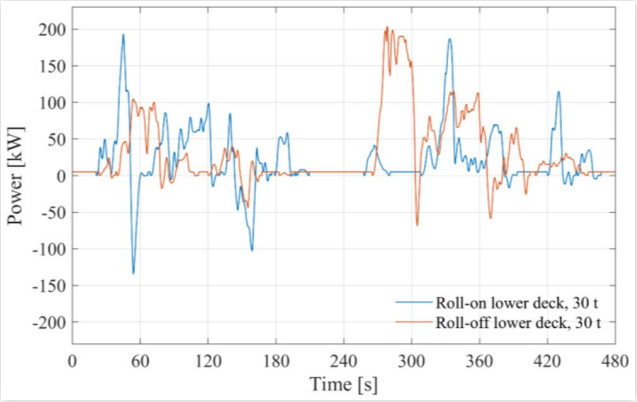

FIGURE 8 HEV total power demand during the driving cycle for cases E and B

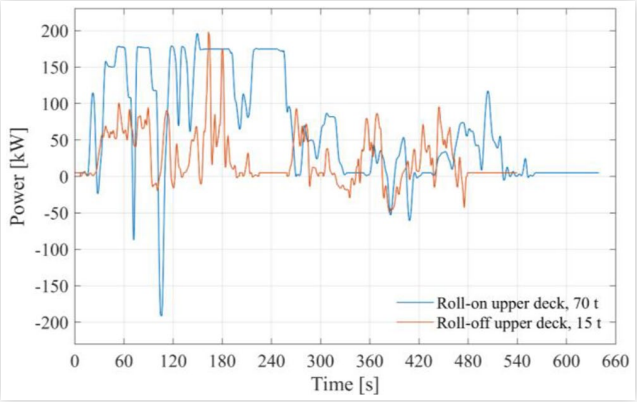

TABLE 4 Results of the duty cycles analysis: mean power, maximum power and energy consumption at the FC/battery output.

Case	$P_{tot,mean}$ [kW]	$P_{tot,max}$ [kW]	E_{tot} [kWh]	Max braking energy recovery [%]
A	39.2	199.8	6.54	7.3
B	24.3	198.3	3.65	9.6
C	20.2	193.2	2.70	14.6
D	29.9	204.0	3.98	5.6
E	62.9	196.5	11.2	4.4
F	26.4	198.3	3.96	14.0
G	38.4	199.8	5.12	7.9
H	24.8	198.3	3.31	9.9

while in Table 4 the main results for the duty cycles analyses, in terms of power and energy requirements, are reported.

The results are consistent, showing that the roll-on operations to the decks above the main deck of the vessel require higher power and energy demands than their respective roll-off operations at the same decks. This is clearly due to the fact that, in those cases, during roll-on the YT climbs the internal ramps of the vessel with being fully loaded, while it carries no trailer when climbing the ramps in roll-off operations. In contrast, the roll-off operation at the lower deck is more demanding than the respective roll-on operation, since in this case the YT climbs the ramp with the loaded trailer during the roll-off operation.

Average mean power output ranges between 20.2 kW (case C) and 62.9 kW (case E). The roll-on of a 70 t trailer to the upper deck of the vessel (case E) is in fact the most demanding operation, as expected. Maximum computed power output are around 200 kW for all cases. It is worth noting that this value is in line with the electric motor requirements.

Table 4 also reports the estimated maximum amount of kinetic energy that can be potentially recovered from regenerative braking, expressed in percentage with respect to the overall tractive energy required to the FC/battery unit during the cycle. Its value stands between 4.4 % (case E) and 14.6 % (case C). Cases B, C, F and H report the highest share of maximum braking energy recovery, given that during these operations the YT experiences several braking events when towing the loaded trailer. These cases correspond also to the less power and energy demanding duty cycles.

Mission Profiles

The designed mission profiles, as reported in Table 3, have been constructed by combining the reference duty cycles. Thus, they have been simulated, by assuming that the vehicle starts its journey with a battery SoC of 90%, in all cases. This value is chosen arbitrarily, assuming that the battery pack can be recharged from the electric grid during the stop of the vehicle at the end of its 6 hours shift.

The instantaneous hydrogen consumption is calculated as:

$$c_{H_2} = \frac{P_{FC}\Delta t}{\eta_{FC}\, LHV_{H_2}} \tag{7}$$

where Δt is the time interval of integration (0.25 s), η_{FC} is the instantaneous fuel cell efficiency, and LHV_{H_2} = 120 MJ/kg is the lower heating value of hydrogen. The SoC profiles are obtained by considering that the SoC variation in time is defined as follows:

$$\begin{cases} \dot{\mathrm{SoC}} = -\dfrac{P_b \eta_{b_c}}{E_b}, & \text{for charging } (P_b < 0) \\ \dot{\mathrm{SoC}} = -\dfrac{P_b}{\eta_{b_d} E_b}, & \text{for discharging } (P_b \geq 0) \end{cases} \tag{8}$$

where η_{b_c} and η_{b_d} are the battery charging and discharging efficiencies, respectively, which are both set equal to 0.97.

First, the most critical scenario, i.e. mission M1, is analyzed. For this case only, the CS mode of operation is set between a different range of SoC levels with respect to the other cases, that is between 40% and 50%, as will be justified later. Figure 9 depicts the obtained battery SoC profile, as a function of time.

From the results presented in Figure 9 it can be readily seen that the fuel cell is not capable of keeping the battery SoC

FIGURE 9 Battery SoC during YT operation for mission M1. The different powertrain modes of operation are highlighted by the horizontal color bar

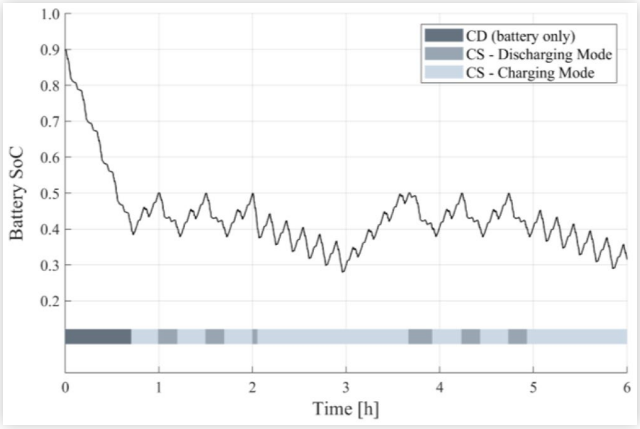

within the predefined range when the YT performs the roll-on operation of 70 t trailers to the upper deck of the vessel. This was indeed expected, since the maximum fuel cell power output (considering also the DC/DC converter efficiency) is lower than the mean power requested to the powertrain during this stage of operation. Therefore, to guarantee the YT continuous operation and the achievement of the target mission, the battery SoC levels for CS must be set such that the battery is never depleted below the lower threshold limit (30%).

Figure 10 shows battery and fuel cell power output profiles, normalized to the maximum power requested to the powertrain, during the most critical stage of operation for mission M1. The fuel cell operates at constant power, with value equal to the CM setpoint, for almost the whole considered stage of operation, while the battery satisfies the peak power requests.

Next, the vehicle performance for all the other mission profiles are evaluated. The results, in terms of battery SoC, are shown in Figures 11 and 12, while in Figure 13 the estimated hydrogen consumption is portrayed as a function of the time of operation, for all the mission profiles.

FIGURE 10 Battery and fuel cell power output, during the most critical stage of operation for mission M1

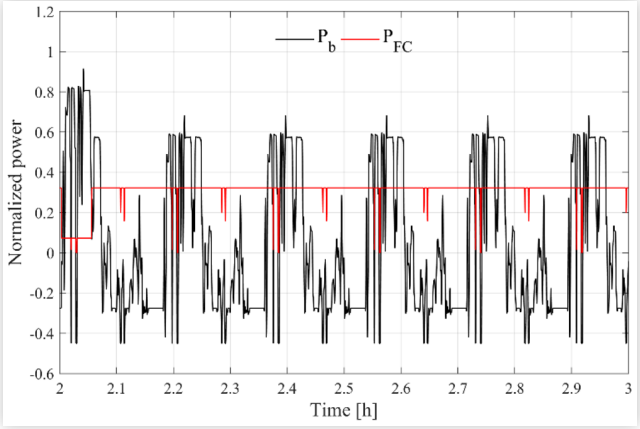

FIGURE 11 Battery SoC, as a function of time, for YT missions M2, M3 and M4

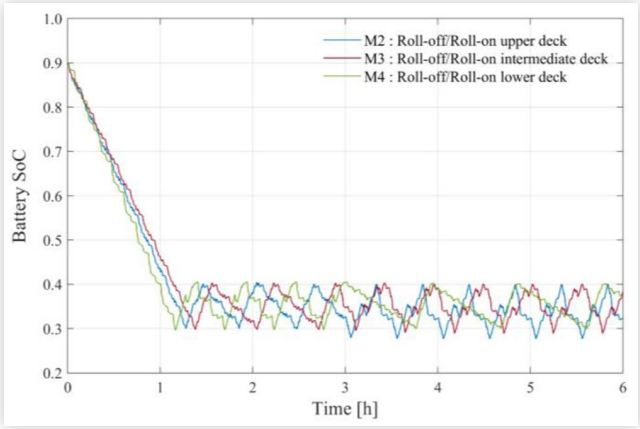

FIGURE 12 Battery SoC, as a function of time, for YT missions M5 and M6

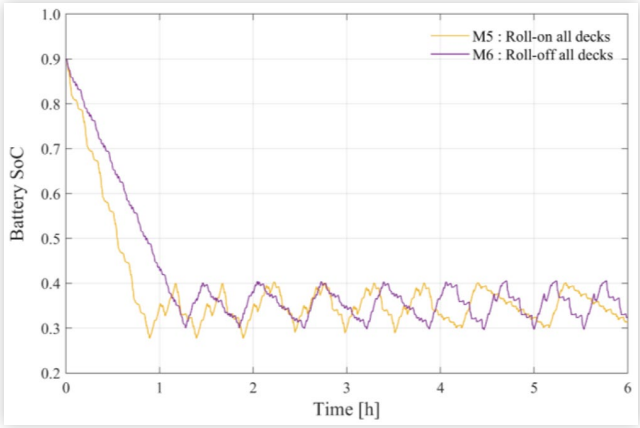

FIGURE 13 Hydrogen consumption during YT operation for all the considered mission profiles

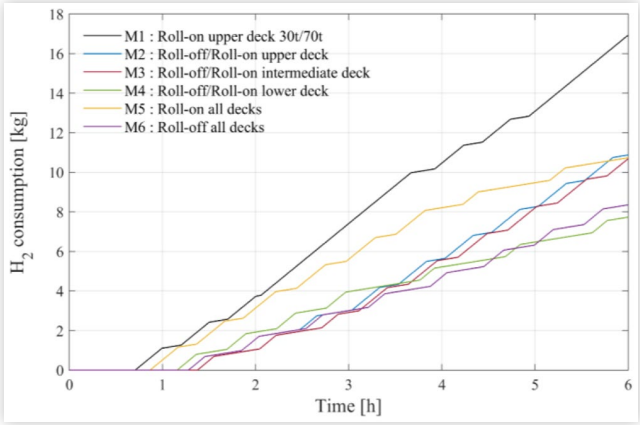

TABLE 5 Main vehicle performance parameters for the considered mission profiles.

N.	H_2 consumption [kg]	Driving range [km]	$\eta_{FC,mean}$	$P_{FC,mean}$
M1	16.9	53.7	0.50	53.6
M2	10.9	54.7	0.51	39.1
M3	10.7	57.1	0.51	39.3
M4	7.7	42.9	0.52	27.9
M5	10.7	51.7	0.51	35.9
M6	8.4	51.6	0.52	30.5

TABLE 7 Diesel consumption for a single ICE vehicle to accomplish the considered mission profiles.

N.	Diesel consumption [L/h]	[kg]
M1	13.25	66.76
M2	9.65	48.62
M3	9.18	46.26
M4	7.37	37.13
M5	9.50	47.87
M6	7.96	40.14

For all the considered scenarios, the HEV achieves the target operation, thus indicating that its powertrain configuration is properly designed. In particular, the battery ensures an adequate all-electric range, with the CD mode of operation lasting for about 1 hour in all cases. Moreover, the CS mode of operation is well suited to keep the battery SoC within its predefined range until the end of the missions. The overall hydrogen consumption is about 16.9 kg for worst case scenario (mission M1), while it ranges between 7.7 kg and 10.9 kg in all the other cases. This indicates that mission M1 would require a tank of larger size than the one designed in [11] (i.e., 12 kg) to be accomplished, while in all the other cases some hydrogen fuel would be saved at the end of the 6 hours operation. These values, along with the other main findings from the analysis, are reported in Table 5.

Despite being based on a non-optimized energy management strategy, the HEV exploits a quite efficient use of the FC (its mean efficiency lies between 0.50 and 0.52 for the analyzed scenarios), which leads to a relatively low consumption of hydrogen.

In order to quantify the beneficial effects on environmental impact at local scale due to the use of a fleet of hydrogen-fueled YTs for RoRo port operations, the emissions related to the original ICE vehicles were estimated. Table 6 reports the computed amount of total energy requested to the Diesel engine YT, for each reference port operation, in comparison with the values retrieved from data acquisition, along with its specific fuel consumption. In particular, the specific fuel consumption was obtained by assuming an average efficiency of 0.35 for the ICE and considering density and lower heating value for Diesel equal to 840 kg/m^3 and 44000 kJ/kg, respectively.

TABLE 6 Energy and fuel consumptions related to the original ICE YT for each reference cycle.

Case	Acquisition $E_{tot,ICE}$ [kWh]	Model	Diesel consumption [L/h]	[kg]
A	6.67	6.67	11.15	1.56
B	4.13	3.85	7.14	0.90
C	3.31	3.03	6.32	0.71
D	4.44	4.03	8.42	0.94
E	-	11.15	17.45	2.61
F	-	4.39	8.15	1.03
G	-	5.28	11.03	1.24
H	-	3.51	7.33	0.82

Basing on the values for each reference port operation, the Diesel consumption for all the YT mission profiles were computed. The result is reported in Table 7.

The average specific fuel consumption for each ICE YT, considering all the defined mission profiles, amounts to 9.48 L/h, which can be assumed as a reference value for the estimation of the in-port emissions on a yearly basis. To this purpose, it is also assumed that the number of docked ships per year is 550 (3 ships every 2 days), each requiring a fleet of 6 YTs. The total number of YT shifts per year employed for RoRo operations is therefore equal to 3300 (i.e. 19800 h of YT operation). This leads to an overall amount of Diesel consumption of roughly 187775 L/year. By considering CO_2 and NOx emission factors equal to 2.67 kg/L_{fuel} and 0.028 kg/L_{fuel} [18], respectively, the estimated in-port emissions result equal to about 501 t/year of CO_2 and 5 t/year of NOx. These amounts correspond to the avoided emissions that would be potentially achieved by adopting hydrogen-fueled vehicles fleets. It is worth noting that the estimated avoided emissions are related only to the direct use of YTs for RoRo port operations, but they do not consider the indirect effect due to the operation of the ship auxiliary systems, such as the ventilation system, which significantly contribute to the overall in-port emissions. The use of these systems could be in fact avoided or mitigated in case of the adoption of hydrogen-fueled YTs, since there would be no pollutants produced by the vehicles inside the ship to remove, thus further reducing the environmental impact in port areas.

To conclude, the presented results show the potential of the hydrogen-fueled heavy-duty vehicle to take the place of the original Diesel engine vehicle in port operations. Besides the clear benefit of zero local emission, other advantages from using hydrogen-fueled fleets include powertrain noise elimination, reduction of the vehicle maintenance costs, improving of the energy management, and increasing of operational efficiency.

Conclusions

In this work, an extensive analysis for the performance evaluation of a heavy-duty hydrogen-fueled YT used in port logistics has been presented. This study follows a previous work from the authors, where a preliminary design of the fuel cell/battery hybrid powertrain for the vehicle was proposed and

assessed by means of a numerical model, ad-hoc developed and validated on data acquired on-field for the original ICE vehicle. In particular, in the present work the same transmission of the original Diesel engine vehicle is considered, i.e. the same gearbox is included in the driveline of the HEV. Thus, multiple mission profiles for the vehicle are designed in order to assess its performance under realistic scenarios.

The results show that the proposed drivetrain solution, along with the choice of an electric motor of reduced size, represents a suitable and effective option.

The hydrogen-fueled YT exhibits interesting energy performance in all the analyzed cases. In fact, it takes advantage from an efficient use of the FC, which provides the base power to the vehicle, while the integrated battery pack follows the transient power demand and recovers energy when braking. By means of this powertrain architecture the HEV successfully accomplishes all the target mission profiles, with a relatively low consumption of hydrogen. The study also demonstrates that the vehicle runs efficiently under critical operating conditions: roll-on of 30 t and 70 t trailers to the upper deck of the vessel. In this case, despite a requested mean power close to the maximum allowed by the fuel cell, the vehicle is capable of accomplishing its task, given a sufficient energy buffer provided by the battery pack and a well-suited on-board energy management.

Finally, the avoided emissions that would be potentially achieved by adopting hydrogen-fueled vehicles fleets instead of the original Diesel engine vehicles have been computed. The benefits in terms of environmental impact are substantial, especially considering that the use of hydrogen-fueled vehicles for RoRo operations would also allow to drastically reduce the indirect emissions due to ship auxiliary systems operation during cargo-handling.

Findings from this study represent a step forward to the development of a benchmark industrial heavy-duty hydrogen-fueled vehicle to be used in real port operations towards a zero-emission scenario.

Acknowledgments

This research has received funding from the Fuel Cells and Hydrogen 2 Joint Undertaking (JU) under grant agreement No 826339, project H2Ports - Implementing Fuel Cells and Hydrogen Technologies in Ports. The JU receives support from the European Union's Horizon 2020 research and innovation programme and Spain, Denmark, Netherlands, Italy.

The authors gratefully acknowledge Grimaldi Euromed SpA for having allowed the measurement campaign at Grimaldi's Terminal in port of Salerno. The authors also gratefully acknowledge Ciro Santoru and all the Manuport (a Terberg Group Company) Operators who have contributed to the vehicle data acquisition.

References

1. European Commission, "Annual Report on CO2 Emissions from Maritime Transport," SWD2020 (82), 2019.
2. International Maritime Organization, "Third IMO GHG Study," 2014.
3. Merk, O., "Shipping Emissions in Ports, International Transport Forum," Discussion Paper N. 2014-20.
4. Balcombe, P., Brierley, J., Lewis, C., Skatvedt, L. et al., "How to Decarbonise International Shipping: Options for Fuels, Technologies and Policies," *Energy Conversion and Management* 182 (2019): 72-88, doi:10.1016/j.enconman.2018.12.080.
5. Di Trolio, P., Di Giorgio, P., Genovese, M., Frasci, E. et al., "A Hybrid Power-Unit Based on a Passive Fuel Cell/Battery System for Lightweight Vehicles," *Applied Energy* 279 (2020): 115734, doi:10.1016/j.apenergy.2020.115734.
6. Lu, X., Wang, P., Meng, L., and Chen, C., "Energy Optimization of Logistics Transport Vehicle Driven by Fuel Cell Hybrid Power System," *International Journal of Hydrogen Energy* (2019): 111887, doi:10.1016/j.enconman.2019.111887.
7. Di Giorgio, P., Di Trolio, P., Jannelli, E., Minutillo, M., et al., Model Based Preliminary Design and Optimization of Internal Combustion Engine and Fuel Cell Hybrid Electric Vehicle, *Energy Procedia*, 148, 2018, 1191-1198, ATI 2018 - 73rd Conference of the Italian Thermal Machines Engineering Association, doi:10.1016/j.egypro.2018.08.022.
8. Ferrara, A., Jakubek, S., and Hametner, C., "Energy Management of Heavy-Duty Fuel Cell Vehicles in Real-World Driving Scenarios: Robust Design of Strategies to Maximize the Hydrogen Economy and System Lifetime," *Energy Conversione and Management* 232 (2021): 113795, doi:10.1016/j.enconman.2020.113795.
9. Lombardi, S., Tribioli, L., Guandalini, G., and Iora, P., "Energy Performance and Well-to-Wheel Analysis of Different Powertrain Solutions for Freight Transportation," *International Journal of Hydrogen Energy* 45 (2020): 12535-12554, doi:10.1016/j.ijhydene.2020.02.181.
10. Kast, J., Vijayagopal, R., Gangloff, J., and Marcinkoski, J., "Clean Commercial Transportation: Medium and Heavy Duty Fuel Cell Electric Trucks," *International Journal of Hydrogen Energy* 42 (2017): 4508-4517, doi:10.1016/j.ijhydene.2016.12.129.
11. Di Ilio, G., Di Giorgio, P., Tribioli, L., Bella, G. et al., "Preliminary Design of a Fuel Cell/Battery Hybrid Powertrain for a Heavy-Duty Yard Truck for Port Logistics," *Energy Conversion and Management* 243 (2021): 114423, doi:10.1016/j.enconman.2021.114423.
12. Sorniotti, A., Subramanyan, S., Turner, A., Cavallino, C. et al., "Selection of the Optimal Gearbox Layout for an Electric Vehicle," *SAE Int. J. Engines* 4, no. 1 (2011): 1267-1280. https://doi.org/10.4271/2011-01-0946.
13. Ehsani, M., Gao, Y., Gay, S., and Emadi, A., *Modern Electric, Hybrid Electric, and Fuel Cell Vehicles: Fundamentals, Theory, and Design* (CRC Press, 2009)
14. Wong, J., *Theory of Ground Vehicles* (John Wiley & Sons, 2008)
15. Terberg Manual, www.terbergbenschop.nl, accessed May 11, 2021, Terberg Benschop B.V.
16. Ballard FCmove™-HD Data Sheet, www.ballard.com, accessed May 11, 2021, Ballard Power Systems.

17. Danfoss EM-PMI375-T800 Data Sheet, www.danfoss.com, accessed May 11, 2021, Danfoss.
18. Gonder, J. and Markel, T., "Energy Management Strategies for Plug-In Hybird Electric Vehilces," SAE Technical Paper 2007-01-0290 (2007). https://doi.org/10.4271/2007-01-0290.
19. EMEP/EEA Air Pollutant Emission Inventory Guidebook 2019, EEA Report N. 13/2019.

Contact Information

Giovanni Di Ilio,
University of Naples "Parthenope", Engineering Department, Centro Direzionale, Isola C4 - 80143 Naples, Italy,
giovanni.diilio@uniparthenope.it

Definitions/Abbreviations

FC - Fuel Cell
YT - Yard Truck
RoRo - Roll-on/Roll-off
HEV - Hybrid Electric Vehicle
EM - Electric Motor
ECU - Engine Control Unit
ICE - Internal Combustion Engine
SoC - State of Charge
CD - Charge Depleting
CS - Charge Sustaining
CM - Charging Mode
DM - Discharging Mode

ISSN 0148-7191